Jordan Journal of Pharmaceutical Sciences, Volume 13, No. 3, 2020

Synthesis, Biological Evaluation and Molecular Modeling Studies of novel 2-[(2,4-dioxo-1,3-thiazolidin-3-yl)acetyl]-*N*-arylhydrazinecarbothioamides as Antibacterial Agents Targeting Alanine Racemase Enzyme

Unni Jayaram[1]*, Mohammed Afzal Azam[1], Ashish Devidas Wadhwani[2], Sameer Kumar Verma[2], Krishnan Rathinasamy[3], Susobhan Mahanty[3]

1 .Department of Pharmaceutical Chemistry, JSS College of Pharmacy, Udhagamandalam- Tamil Nadu, India (A Constituent College of JSS Academy of Higher Education & Research, Mysuru).
2. Department of Pharmaceutical Biotechnology, JSS College of Pharmacy, Udhagamandalam- 643001, Tamil Nadu, India (A Constituent College of JSS Academy of Higher Education & Research, Mysuru).
3. School of Biotechnology, National Institute of Technology, Calicut, Kerala, India.

ABSTRACT

Antibiotics play a prominent role in modern health care. Although, their role focuses on treatment of minor as well as serious infections, decreased antibiotic effectiveness has emerged as a major threat. Currently, the prime focus of researchers are to make structurally novel class of antibiotics with novel mechanism of action. The alanine racemase (AlaR) is a ubiquitous prokaryotic enzyme that provides peptidoglycan precursor D-alanine (D-Ala) for bacterial cell wall synthesis. The aim of present study is to identify some novel AlaR inhibitors with the ability to act as potent antibacterial agents. Herein we report five novel 2-[(2,4-dioxo,1,3-thiazolidin-3-yl)acetyl]-*N*-arylhydrazinecarbothioamides (**5-9**) which were synthesized and characterized by spectral data. All compounds were screened for their antibacterial activity and *Geobacillus stearothermophilus* alanine racemase enzyme (AlaR) inhibitory action. Compound **8** exhibited significant activity against the tested strains of bacteria when compared to the standard drug methicillin. In AlaR inhibition assay, the tested compound **8** showed maximum inhibitory activity (IC_{50} = 0.5 µM) compared to the standard drug D-cycloserine (IC_{50} = 0.93 µM) and inhibitor *O*-acetyl-L-serine (IC_{50} = 4.2 µM). The *in silico* study showed that substitution of chlorine atom on the phenyl ring in case of compound **8** increased the hydrophobic interaction at the catalytic pocket resulting in high AlaR inhibitory action. The study suggests that the synthesized compound **8** can be considered as a promising antibacterial agent and a potent lead molecule for further antibacterial drug discovery and development.

Keywords: 1,3-thiazolidine-2,4-dione, alanine racemase, antibacterial activity, molecular modeling, synthesis, cytotoxicity.

INTRODUCTION

The Gram-positive bacterium *Staphylococcus aureus* (*S. aureus*) is an opportunistic microorganism that causes wide variety of diseases ranging from minor skin infections to more fatal conditions such as pneumonia, meningitis and septicaemia. It is a leading cause of nosocomially acquired infections mainly caused by the existence of methicillin- and glycopeptide antibiotic-resistant strains.[1] Emergence of methicillin resistant *Staphylococcus aureus* (MRSA) strains such as Mu50, which are also resistant to vancomycin[1] further complicated the problem. Linezolid and daptomycin are the drugs currently used for treating vancomycin resistant *S. aureus* infections. However, these antibiotics are associated with some serious side effects over prolonged use,[2,3] and resistance to both has been observed.[4,5] This emphasizes the need for the development of novel antibacterial agents targeting the bacterial enzymes which

* jayaramkvt@gmail.com
Received on 7/3/2019 and Accepted for Publication on 11/1/2020.

act by different mechanism of action. Alanine racemase (AlaR) is a bacterial enzyme which catalyzes the racemization of L-alanine to D-alanine, an essential component for the synthesis of bacterial cell wall peptidoglycan. The co-factor pyridoxal-5′-phosphate (PLP) plays the major role in this racemization mechanism.[6-9]

Being ubiquitously distributed in bacteria and generally absent in higher eukaryotes, this enzyme is considered to be a potential target for the antibacterial drug discovery.[10] However, in some bacteria like *Listeria monocytogenes*, synthesis of D-alanine occur by another pathway.[9] High resolution crystal structures of AlaR catalytic domain has been solved from *S. aureus*,[11] *Mycobacterium tuberculosis*,[12] *Geobacillus stearothermophilus*,[13] *Bacillus anthracis*,[14] *Enterococcus faecalis*,[15] *Streptococcus pneumonia*,[16] *Clostridium difficile*,[17] *Streptomyces coelicolor*,[18] making it possible for the structure based design of new AlaR inhibitors. The crystal structure of *S. aureus* AlaR from the antibiotic-resistant Mu50 strain has been solved to 2.15 Å resolution (PDB-ID: 4A3Q).[11] Superpositions of *S. aureus* AlaR C-*α*-atom of active-site residues showed high structural similarity with the active site residues of *G. stearothermophilus* AlaR (70%) and *B. anthracis* AlaR (68%) and share less structural similarity with *Pseudomonas aeruginosa* AlaR (47%) and *M. tuberculosis* AlaR (51%).[11]

Structural analogues of D-alanine[19] have been investigated as AlaR inhibitors. But these inhibitors were observed to be non-specific, also acting on other PLP-containing enzymes, including those present in humans.[11] Among these known AlaR inhibitors, only D-cycloserine has been approved clinically, but its use is limited due to the adverse effects arising from the lack of target specificity.[20] Apart from D-cycloserine, several other AlaR inhibitors are known that includes the natural antibiotics *O*-carbamoyl-D-serine,[21] and alanine analogues such as alanine phosphonate,[19] *β*-fluoroalanine, *β*-chloroalanine[22] and *β*,*β*,*β*-trifluoroalanine.[23] D-cycloserine is marketed for the treatment of *M. tuberculosis* infection. It has limited use as it is associated with resistance and severe central nervous system toxicity due to the inhibition of human enzymes that utilize PLP as a co-factor.[20,24] Other inhibitors which are not used clinically such as alanine phosphonate and propionate also target PLP and thereby suffer from the same lack of specificity.[25,26] This emphasizes the need for the development of new inhibitors for alanine racemase with greater specificity, which may cause less toxicity in humans. Moreover, the 1,3-thiazolidine-2,4-dione scaffold is known to have promising antibacterial activity.[27-32] Furthermore, phenyl hydrazinecarbothioamide derivatives are also shown to be competent antibacterial agents.[33,34] On the basis of above findings, we aimed to evaluate the potency of some novel 2-[(2,4-dioxo-1,3-thiazolidin-3-yl)acetyl]-*N*-arylhydrazinecarbothioamides as AlaR enzyme inhibitors and antibacterial agents. Molecular docking of all synthesized compounds and molecular dynamics simulation of most potent molecule **8** were performed at the catalytic pocket of *S. aureus* Mu50 strain alanine racemase (PDB-ID: 4A3Q) to get insight into the molecular mechanism of interactions and possible binding modes of these molecules with the protein.

Results and discussion

Synthesis

Synthesis of 1,3-thiazolidine-2,4-dione (**1**)[35]

Melting point (mp): 123-125 °C (lit.[35] mp: 120-125 °C). Yield 90%. TLC solvent system: acetone: dichloromethane: petroleum ether (2:1:1). R_f value (0.62). FT-IR (KBr, cm^{-1}): 3469 (>NH), 2948 (-CH_2), 1736, 1650 (>C=O), 1226 (C-N), 716 (C-S-C).

Synthesis of potassium salt of 1,3-thiazolidine-2,4-dione(**2**)[36]

Mp: 245-247 °C (lit.[36] mp: 247-250 °C). Yield 80%. TLC solvent system: acetone: dichloromethane: petroleum ether (2:1:1). R_f value (0.60). FT-IR (KBr, cm^{-1}): 2928 (-CH_2), 1691, 1654 (>C=O), 1230 (C-N), 703 (C-S-C).

Synthesis of ethyl (2,4-dioxo-1,3-thiazolidin-3-yl) acetate(3) [36]

Boiling point (bp): 108-110 °C (lit.[36] bp: 107-110 °C). Yield 65%. TLC solvent system: acetone: dichloromethane: petroleum ether (1:1:2). R_f value (0.57). FT-IR (KBr, cm^{-1}): 2982 (-CH_3), 2936 (-CH_2), 1735, 1728, 1673 (>C=O), 1230 (C-N), 750 (C-S-C).

Synthesis of 2-(2,4-dioxo-1,3-thiazolidin-3-yl) acetohydrazide (4)

Mp: 180-184 °C. Yield 90%. TLC solvent system: methanol: acetone: petroleum ether (1:1:1). R_f value (0.64). FT-IR (KBr, cm^{-1}): 3318, 3253 (>NH), 2937 (-CH_2), 1787, 1729, 1654 (>C=O), 1228 (C-N), 710 (C-S-C). ^{1}H NMR (400 MHz, DMSO-d_6, δ ppm): 7.88 (s, 1H, -NH), 4.65 (s, 2H, -CH_2 aliphatic), 3.85 (s, 2H, -NH_2), 3.36 (s, 2H, -CH_2 cyclic). ^{13}C NMR (DMSO-d_6, δ ppm): 170.14, 161.14, 157.28, 44.42, 38.80.

***N*-(4-chlorophenyl)-2-[(2,4-dioxo-1,3-thiazolidin-3-yl)acetyl]hydrazinecarbothioamide (5)**

Solvent crystallization: acetone. Mp: 202-204 °C. Yield 72%. TLC solvent system: methanol: petroleum ether (1:2). R_f value (0.52). FT-IR (KBr, cm^{-1}): 3318, 3253 (-NH), 2937 (-CH_2), 1780, 1729, 1652 (>C=O), 1600 (ArC=C), 1311 (-C=S), 1229 (C-N), 810 (para substituted benzene), 711 (C-Cl), 606 (C-S-C). ^{1}H NMR (400 MHz, DMSO-d_6, δ ppm): 10.52 (s, 1H, -NH), 10.04 (s, 1H, -NH) 8.29 (s, 1H, -NH), 7.89-6.98 (m, 4H, ArH), 4.63 (s, 2H, -CH_2 aliphatic), 3.36 (s, 2H, >CH_2 cyclic). ^{13}C NMR (DMSO-d_6, δ ppm): 169.95, 169.92, 169.31, 157.21, 147.41, 132.48, 129.67, 128.32, 44.46, 39.49. GC-MS (EI-TOF) m/z calculated for $C_{12}H_{11}ClN_4O_3S_2$: 358.82. Found: m/z 356.2 ($M^{+\cdot}$-3), 323.1, 251.2, 178.1, 135.1 (base peak), 107.1, 77.1. Anal. Calcd. for $C_{12}H_{11}ClN_4O_3S_2$: C, 40.17; H, 3.09; N, 15.61; S, 17.87. Found: C, 40.23; H, 3.11; N, 15.25; S, 17.90.

2-[(2,4-dioxo-1,3-thiazolidin-3-yl)acetyl]-*N*-phenylhydrazinecarbothioamide (6)

Solvent crystallization: ethanol. Mp: 194-196 °C. Yield 81%. TLC solvent system: methanol: petroleum ether (1:2). R_f value (0.53). FT-IR (KBr, cm^{-1}): 3318, 3253 (-NH), 3030 (ArH), 2937 (-CH_2), 1788, 1729, 1652 (>C=O), 1616 (ArC=C), 1311 (-C=S), 1228 (C-N), 710 (C-S-C), 763, 710 (mono substituted benzene). ^{1}H NMR (400 MHz, DMSO-d6, δ ppm): 10.41 (s, 1H, -NH), 10.02 (s, 1H, -NH), 8.57 (s, 1H, -NH), 7.26-7.09 (m, 5H, ArH), 4.61 (s, 2H, -CH_2 aliphatic), 3.37 (s, 2H, >CH_2 cyclic). ^{13}C NMR (DMSO-d_6, δ ppm): 172.51, 169.92, 169.31, 159.22, 147.41, 132.48, 129.67, 128.32, 44.46, 39.49. GC-MS (EI-TOF) m/z calculated for $C_{12}H_{12}N_4O_3S_2$: 324.37. Found: m/z 321.21 ($M^{+\cdot}$-3), 251, 228.1, 135.0 (base peak), 116.1, 93.1, 66.1. Anal. Calcd. for $C_{12}H_{12}N_4O_3S_2$: C, 44.43; H, 3.73; N, 17.27; S, 19.77. Found: C, 44.22; H, 3.25; N, 17.09; S, 19.42.

2-[(2,4-dioxo-1,3-thiazolidin-3-yl)acetyl]-*N*-(4-hydroxyphenyl) hydrazinecarbothioamide (7)

Solvent crystallization: ethanol. Mp: 212-214 °C. Yield 82%. TLC solvent system: methanol: petroleum ether (1:2). R_f value (0.48). FT-IR (KBr, cm^{-1}): 3467 (-OH), 3318, 3253 (-NH), 3010 (ArH), 2937 (-CH_2), 1787, 1728, 1651 (>C=O), 1577 (ArC=C), 1311 (-C=S), 1228 (C-N), 710 (C-S-C), 841 (para substituted benzene). ^{1}H NMR (400 MHz, DMSO-d_6, δ ppm): 10.28 (s, 1H, -NH), 10.02 (s, 1H, -NH), 8.22 (s, 1H, -NH), 7.89 (s, 1H, -OH), 7.68-7.09 (m, 4H, ArH), 4.63 (s, 2H, -CH_2 aliphatic), 3.35 (s, 2H, >CH_2 cyclic). ^{13}C NMR (DMSO-d_6, δ ppm): 172.51, 169.88, 169.22, 157.18, 147.42, 132.52, 129.66, 128.21, 44.45, 39.53. GC-MS (EI-TOF) m/z calculated for $C_{12}H_{12}N_4O_4S_2$: 340.37. Found: m/z 341.0 ($M^{+\cdot}$+1), 255.8 (base peak), 223.8, 191.8, 159.9, 127.9, 95.9, 64.0. Anal. Calcd. for $C_{12}H_{12}N_4O_4S_2$: C, 42.34; H, 3.55; N, 16.46; S, 18.84. Found: C, 42.38; H, 3.42; N, 16.40; S, 18.90.

***N*-(3-chlorophenyl)-2-[(2,4-dioxo-1,3-thiazolidin-3-yl)acetyl]hydrazinecarbothioamide (8)**

Solvent crystallization: ethanol. Mp: 156-158 °C. Yield 69%. TLC solvent system: methanol: petroleum ether (1:2). R_f value (0.82). FT-IR (KBr, cm^{-1}): 3344, 3236 (-NH), 3055 (ArH), 2988 (-CH_2), 1794, 1721, 1645 (>C=O), 1595 (ArC=C), 1335 (-C=S), 1247 (C-N), 702 (C-S-C), 724 (Ar-Cl). ^{1}H NMR (400 MHz, DMSO-d_6, δ ppm): 10.50 (s, 1H, -NH), 10.04 (s, 1H, -NH) 8.29 (s, 1H, -NH), 7.90-7.13 (m, 4H, ArH), 4.64 (s, 2H, -CH_2 aliphatic), 3.38 (s, 2H, >CH_2 cyclic). ^{13}C NMR (DMSO-d_6, δ ppm): 169.92, 169.31, 157.21, 154.39, 140.11, 139.65, 132.48, 129.67, 125.43, 124.30, 44.85, 39.49. GC-MS (EI-TOF) m/z calculated for $C_{12}H_{11}ClN_4O_3S_2$: 358.82. Found: m/z 356.2 ($M^{+\cdot}$-3), 321.1, 215.0 (base peak), 182.1, 170, 154, 127, 111, 75.1, 63.1. Anal. Calcd. for $C_{12}H_{11}ClN_4O_3S_2$: C, 40.17; H, 3.09; N, 15.61; S, 17.87. Found: C, 40.42; H, 3.53; N, 15.37; S, 17.49.

2-[(2,4-dioxo-1,3-thiazolidin-3-yl)acetyl]-*N*-(4-methylphenyl) hydrazinecarbothioamide (9)

Solvent crystallization: ethanol. Mp: 154-156 °C. Yield 64%. TLC solvent system: methanol: petroleum ether (1:1). R_f value (0.64). FT-IR (KBr, cm^{-1}): 3392, 3253 (-NH), 2990 (-CH_2), 1782, 1731, 1677 (>C=O), 1613 (ArC=C), 1317 (-C=S), 1213 (C-N), 702 (C-S-C), 813 (para substituted benzene). ^{1}H NMR (400 MHz, DMSO-d6, δ ppm): 10.87 (s, 1H, -NH), 9.65 (s, 1H, -NH) 8.24 (s, 1H, -NH), 7.52-7.07 (m, 4H, ArH), 4.51 (s, 2H, -CH_2 aliphatic), 3.37 (s, 2H, >CH_2 cyclic), 2.36 (s, 3H, -CH_3). ^{13}C NMR (DMSO-d_6, δ ppm): 172.95, 169.92, 169.31, 155.65, 138.84, 136.77, 129.67, 128.29, 40.15, 39.52, 20.77. GC-MS (EI-TOF) m/z calculated for $C_{13}H_{14}N_4O_3S_2$: 338.40. Found: m/z 340.9 ($M^{+\cdot}$+2), 286.2, 195.1 (base peak), 162, 134.1, 106.1, 91.1, 77.1. Anal. Calcd. for $C_{13}H_{14}N_4O_3S_2$: C, 46.14; H, 4.17; N, 16.56; S, 18.95. Found: C, 46.25; H, 4.22; N, 16.49; S, 18.92.

Chemistry

The procedure adopted for the synthesis of title compounds **5-9** is outlined in Scheme 1. The % yield of the synthesized compound (**5-9**) is presented in Table 1. The structures of all synthesized compounds were characterized by FT-IR, ^{1}H NMR, ^{13}C NMR, mass spectra and elemental analysis (Figure 1 and Supplementary Figures S2 and S3). In the Infra-red (IR) spectrum of compound **1**, the characteristic -NH band at 3469 cm^{-1} and carbonyl stretch at 1650 and 1736 cm^{-1} were observed.[35] The formation of 1,3-thiazolidine-2,4-dione potassium salt (**2**), was supported by the disappearance of -NH band observed in compound **1**. The intermediate compound **3**, exhibited the characteristic carbonyl stretch at 1673, 1728 and 1735 cm^{-1}, C-N stretching at 1230 cm^{-1} and C-S stretching at 1027 cm^{-1}. The characteristic two intense IR bands at 3253 and 3318 cm^{-1} for -NH groups, which were absent in **3**, supported the formation of intermediate compound **4** (Figure 2). In addition, three prominent stretching bands for >C=O groups at 1654, 1729 and 1787 cm^{-1} were also observed. The ^{1}H NMR spectrum of the compound **4** showed a singlet at δ 7.88 ppm corresponding to -CONH proton. A singlet observed at δ 4.65 ppm is for protons from -CH_2 group and the singlet observed at δ 3.85 ppm is ascribed for two protons of -NH_2 group of the acetohydrazide side chain. The >CH_2 group in the thiazolidinedione ring showed the singlet at δ 3.36 ppm. In the ^{13}C NMR spectrum of **4**, signals at δ 170.14, 161.14, 157.28, 44.42 and 38.80 ppm, justified the total number and nature of carbon atoms in the chemical structure.[50] In the IR spectrum of compound $\mathbf{D_1}$, bands were observed at 2346 cm^{-1} (-N=C=S), and 830 cm^{-1} (Ar-Cl).[51] The title compounds **5-9**, exhibited characteristic IR bands at 3236-3392 cm^{-1} for -NH and 1651-1794 cm^{-1} for >C=O group.[50] The disappearance of IR band in the range 2100-2400 cm^{-1} corresponding to the -N=C=S group confirmed the formation of title compounds. In the ^{1}H NMR spectrum of **8**, singlet signals at δ 8.29, 10.04 and 10.50 ppm were assigned to three -NH groups of hydrazine carbothioamide linker. The multiplet observed at δ 7.13-7.90 ppm were assigned to four aromatic protons of *m*-Cl-benzene in the compound. The >CH_2 group in thiazolidinedione ring showed a singlet at δ

3.84 ppm. While, the aliphatic -CH_2 group in the carbon chain linker was characterized by another singlet for two protons at δ 4.64 ppm.[50] The ^{13}C NMR spectrum (in DMSO-d_6) of compound **8** showed two signals at δ 157.21 and 169.31 ppm which were assigned to the carbonyl carbons of thiazolidin-2,4-dione nucleus. The -C=S, thioamide carbon in hydrazine carbothioamide linker was characterized by signal at δ 169.92 ppm. The signal at δ 154.39 ppm corresponds to the -CONH- group of hydrazine carbothioamide linker. The signals observed at δ 124.30, 125.43, 129.67, 132.48, 139.65 and 140.11 ppm were assigned to the benzene carbons of *m*-Cl benzene ring. The -CH_2 group attached to the thiazolidinedione ring showed signal at δ 44.85 ppm while signal at δ 39.49 ppm was ascribed to the thiazolidinedione ring -CH_2 fragment.[50] The mass spectrum of compound **8** showed an [M^{+}-3] peak at m/z 356.2 which is complemented by the calculated molecular weight of 358.82. ($C_{12}H_{11}ClN_4O_3S_2$). The physico-chemical properties of the synthesized molecules are summarized in Table 1.

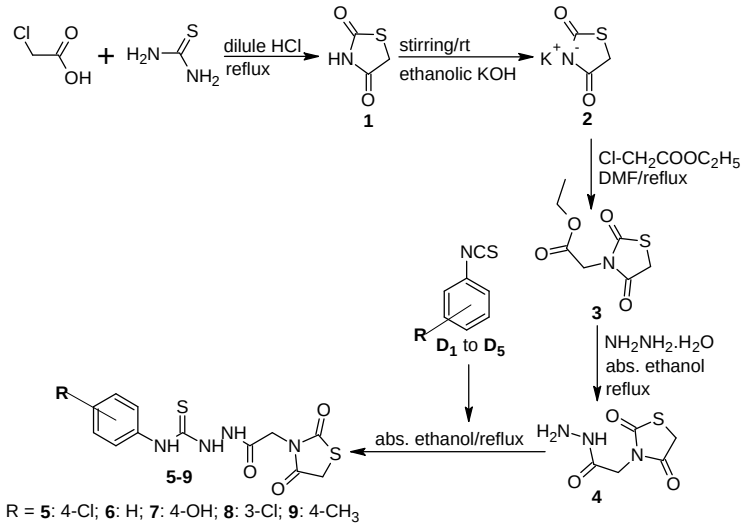

Scheme 1. Synthetic route for the synthesis of titled compounds 5-9.

Table 1. The physicochemical properties of the synthesized compounds 5-9.

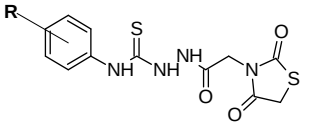

Compound	R	Molecular formula	Molecular weight	Melting point (°C)	Solvent of crystallization	Yield*(%)
5	4-Cl	$C_{12}H_{11}ClN_4O_3S_2$	358.82	202-204	acetone	72
6	H	$C_{12}H_{12}N_4O_3S_2$	324.38	194-196	ethanol	81
7	4-OH	$C_{12}H_{12}N_4O_4S_2$	340.38	212-214	ethanol	82
8	3-Cl	$C_{12}H_{11}ClN_4O_3S_2$	358.82	156-158	ethanol	69
9	4-CH_3	$C_{13}H_{14}N_4O_3S_2$	338.41	154-156	ethanol	64

*Isolated Yield

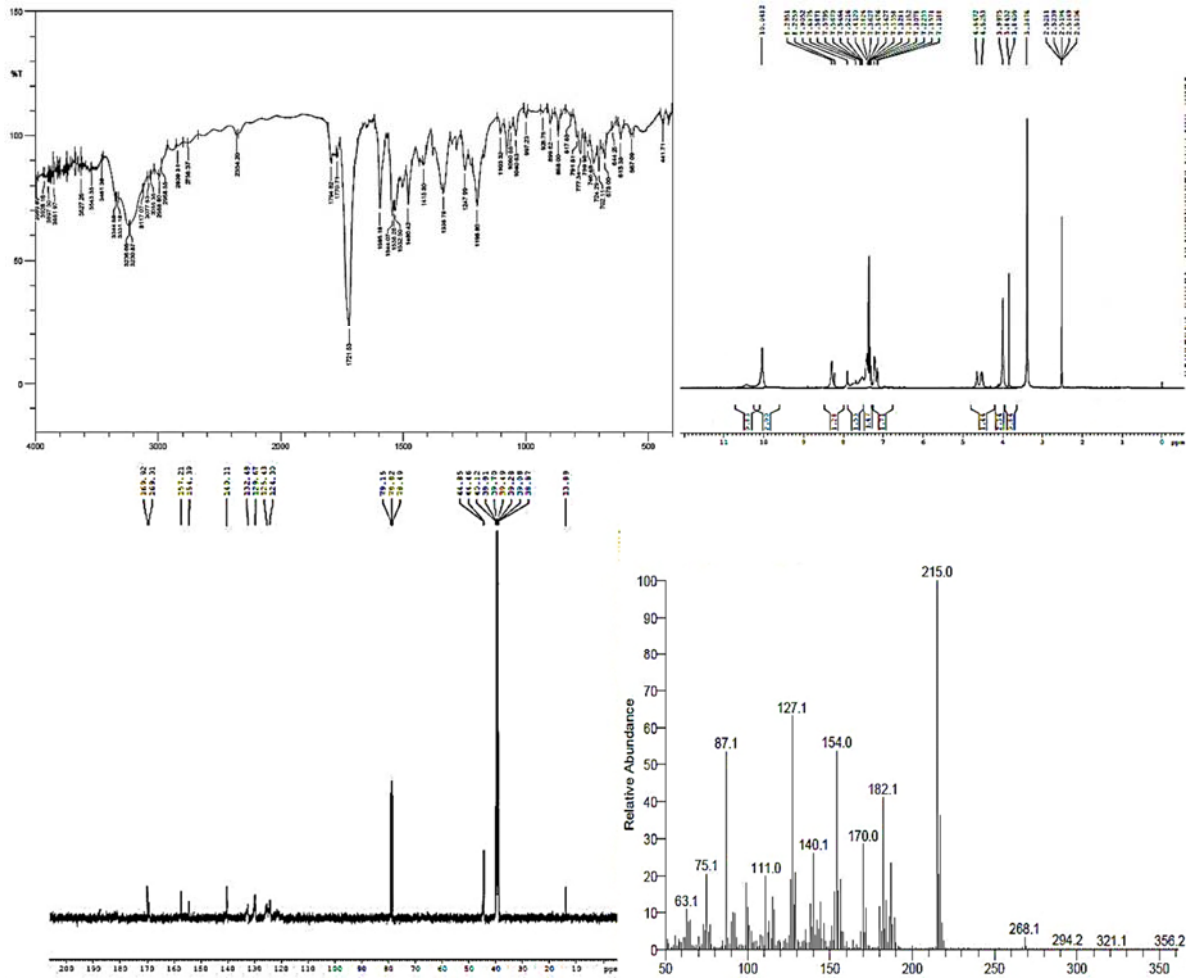

Figure 1. The a) FTIR, b) ^{1}H NMR, c) ^{13}C NMR, and d) Mass spectra of the compound 8.

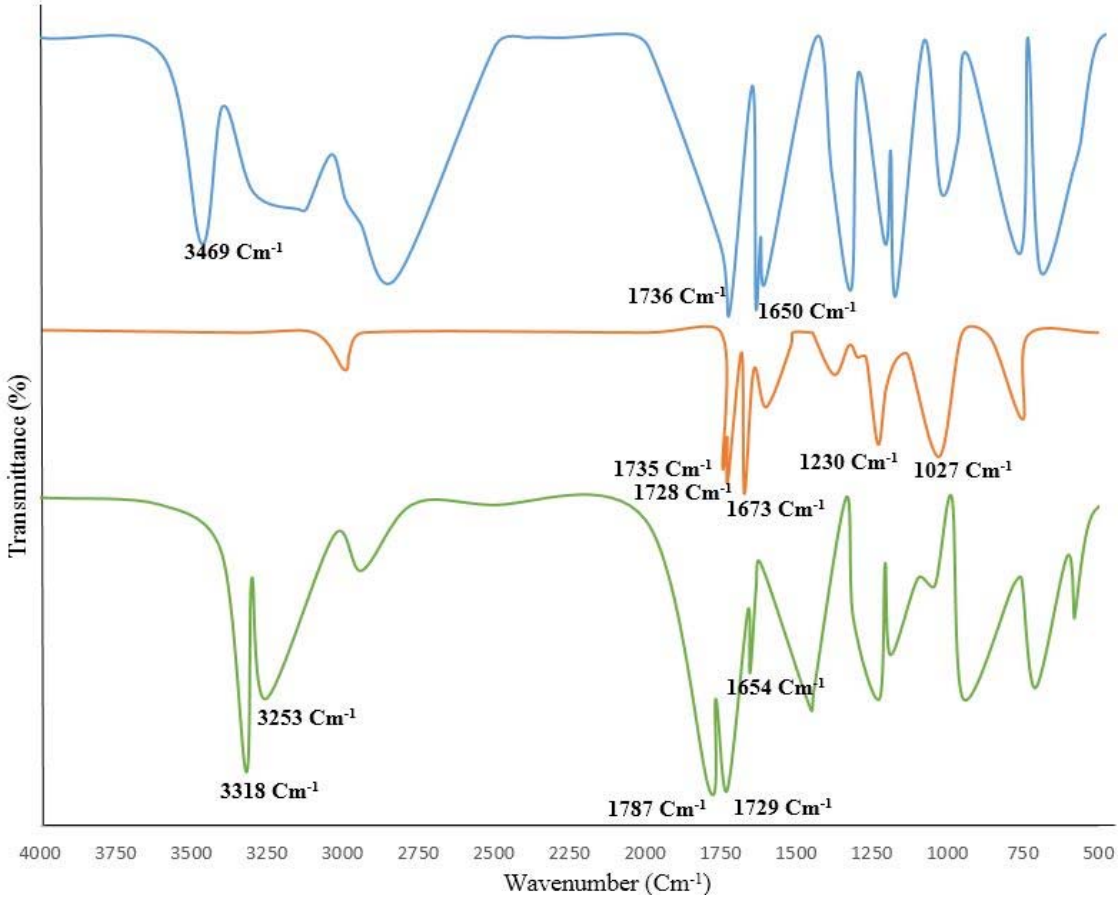

Figure 2. The overlay of the FTIR spectra of Compounds 1 (blue), 3 (red) and 4 (green).

Determination of minimum inhibitory concentration (MIC)

The MIC values in µg/ml of the synthesized molecules and standard drugs are listed in Table 2. The MIC values of the test compounds were in the range 3.125 to 25 µg/ml. The test compound **8** showed promising activity against the tested strain of *B. subtilis* NCIB 8054 (MIC of 3.125 µg/ml) compared to the standard drug methicillin (MIC of 6.25 µg/ml) and amoxicillin (MIC of 1.56 µg/ml). Compound **8** also showed moderate activity against the tested strains of *S. aureus* (ATCC 6538P, ATCC 25923 and ATCC 29213) (MIC of 6.25 µg/ml) in comparison to the standard drug methicillin (MIC of 3.125 µg/ml). Compound **8**, along with **5** and **6**, exhibited moderate activity against *P. aeruginosa* ATCC 19429 (MIC of 6.25 µg/ml) and *Escherichia coli* (*E. coli*) ATCC 8739 (MIC of 6.25 µg/ml) compared to the methicllin (MIC of 1.56 µg/ml). Compound **9** was found to be less active against all tested bacterial strains. The results suggest that compound possessing 3-chlorophenyl ring attached to hydrazine carbothioamide linker (in **8**) enhances antibacterial activity against the selected strains, especially towards *B. subtilis* NCIB 8054. It is also evident that 4-hydroxyphenyl ring attached to hydrazine carbothioamide linker (in **7**) also increased the antibacterial activity against *P. aeruginosa* ATCC 19429. However, hydrazine carbothioamide linker with 4-methylphenyl ring attachment (in **9**) diminished the antibacterial activity.

Table 2. Determination of the minimum inhibitory concentration of the synthesized molecules and standard drugs against selected strains of microorganisms.

Compound	Minimum inhibitory concentration [µg/ml][a]					
	S.a [b]	***S.a*** [c]	***S.a*** [d]	***B.s*** [e]	***E.c*** [f]	***P.a*** [g]
5	6.25	12.5	12.5	6.25	6.25	62.5
6	6.25	6.25	6.25	6.25	6.25	6.25
7	25	12.5	25	6.25	12.5	3.125
8	6.25	6.25	6.25	3.125	6.25	6.25
9	25	25	25	25	25	25
Methicillin	3.125	3.125	3.125	6.25	1.56	1.56
Amoxicillin	3.125	3.125	1.56	1.56	3.125	1.56

[a]Average of three independent determinants.

[b]*S.a.*: *Staphylococcus aureus* (ATCC 6538P); [c]*S.a.*: *Staphylococcus aureus* (ATCC 25923); [d]*S.a.*: *Staphylococcus aureus* (ATCC 29213); [e]*B.s.*: *Bacillus subtilis* (NCIB 8054); [f]*E.c.*: *Escherichia coli* (ATCC 8739); [g]*P.a.*: *Pseudomonas aeruginosa* (ATCC 19429).

AlaR enzyme inhibitory assay

The *in vitro* AlaR enzyme inhibitory assay was performed for the synthesized molecules. The IC_{50} values were determined for the molecules. The test compounds **5-9** and the standard drugs (D-cycloserine and *O*-acetyl-L-serine) were evaluated at 0.19-100 µg/ml in a two-fold serial dilution manner. The tested compound **8** showed maximum inhibitory activity (IC_{50} = 0.5 µM) against *G. stearothermophilus* AlaR compared to the standard drugs D-cycloserine (IC_{50} = 0.93 µM) and *O*-acetyl-L-serine (IC_{50} = 4.2 µM), while compound **7** showed moderate inhibitory activity (IC_{50} = 1.8 µM). Compound **6** was observed to be low active (IC_{50} = 47 µM), while compounds **5** and **9** exhibited IC_{50} value more than 100 µM. When we analyzed the results, we found that, 3-chlorophenyl ring attached to hydrazine carbothioamide linker further attached to thiazolidin-2,4-dione ring (in **8**) plays crucial role in imparting the AlaR inhibitory activity. However, the presence of 4-chloro (in **5**) and 4-methyl (in **9**) groups attached to the phenyl ring diminished their AlaR inhibitory activity. Even phenyl ring attached to hydrazine carbothioamide linker without any substitution over aryl ring failed to exhibit any significant activity.

Compound cytotoxicity studies by sulforhodamine B assay

Cells were treated with 50, 100 and 150 µM concentrations of compounds and showed concentration dependent effect on the viability of the cell line. The cell line showed more than 50% cell viability even at higher concentration of 150 µM (Figure 3). From the obtained result it can be inferred that compounds did not possess significant effect on the cell viability and have minimal cytotoxic effect on the cell line even at a higher concentration.

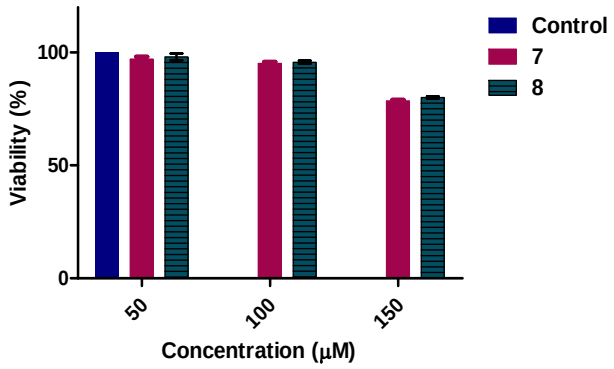

Figure 3. The effect of synthesized compounds **7** and **8** on the viability of the mouse fibroblast cell line L929.

Molecular docking and binding free energy (MM-GBSA) calculation

The results of extra-precision (XP) docking and binding free energy calculation by molecular mechanics generalized born surface area (MM-GBSA) approach is summarized in Table 3. For compounds **5-9**, Glide docking score were in the range -3.93 to -5.79 kcal mol^{-1}. Hydrogen bonding and π-π stacking interactions were observed with key binding site residues Lys39, His168, Phe169, Cys171 and Ala172, however no interaction was observed with co-factor PLP1039. In compound **7** (IC_{50} = 1.8 μM), the side chain carbonyl oxygen of Phe169 accepted a hydrogen bond from the OH group (>C=O···HO, 2.00 Å) present on position four of phenyl ring (Figure 4a). This hydroxyl group oxygen also accepted a hydrogen bond from the side chain -NH of Cys171 (HN···OH, 1.93 Å). The carbonyl oxygen of -CH_2CONHNHCS- fragment of this compound showed hydrogen bonding interaction with imidazole ring -NH of His168 (rNH···O=C<, 1.67 Å). The van der Waals (ΔG_{vdW}) energy term for compound **7** was found to be -42.18 kcal mol^{-1}. It was also found that the position of Cl substituent on the phenyl ring in compounds **5** and **8** highly influenced the AlaR inhibitory activity. In case of compound **8** (IC_{50} = 0.5 μM) the carbonyl oxygen of -CH_2CONHNHCS- fragment showed hydrogen bonding interaction with -NH of Lys39 (>C=O···HN, 2.02 Å) while sulfur of thiocarbonyl >C=S formed hydrogen bond with imidazole ring NH of His168 (rNH···S=C<, 2.46 Å) (Figure 4b). Position two carbonyl oxygen of 2,4-thiazolidinedione ring accepted a water mediated hydrogen bond from -NH of Lys39 (>C=O···NH, 1.82 Å). The van der Waals (ΔG_{vdW}) energy term for compound **8** was found to be -47.22 kcal mol^{-1}. In exception to this, for compound **5** having chloro substitution on position four in phenyl ring caused diminished activity. Interestingly the mere change in the position of Cl substituent to third position of the phenyl ring caused promising AlaR inhibitory activity in compound **8.** In compound **5**, the position two carbonyl oxygen of 2,4-thiazolidinedione ring accepted two hydrogen bonds, one from -NH of Cys171 (>C=O···NH, 1.70 Å) and the other from -NH of Ala172 (>C=O···NH, 1.90 Å). This huge difference in AlaR inhibitory activity may be attributed to the fact that the compound **5** failed to show any prominent interaction with Lys39 residue when compared to compound **8**. The Lys39 residue at the catalytic binding pocket plays crucial role in the racemization mechanism. It is evident from docking result that the compounds **7** and **8** have stable orientation within the catalytic pocket of *S. aureus* AlaR enzyme (PDB-ID: 4A3Q) and are capable of forming stable interactions with key binding site residues. The binding free energy of compounds **5-9** calculated by the MM-GBSA approach ranged between -21.59 to -80.85 kcal mol^{-1} (Table 3). It is evident from result that van der Waals (ΔG_{vdW}) and non-polar solvation (ΔG_{Lipo}) energy terms strongly favor, while covalent energy (ΔG_{Cov}) and electrostatic solvation (ΔG_{Solv}) energy terms disfavor the ligand binding in the active site of 4A3Q. In compounds **5**, **7** and **9**, Coulomb energy term moderately (ΔG_{Coul}: -6.48 to -29.53 kcal mol^{-1}) favored the ligand binding, while in compounds **6** and **8**, this energy term opposes the ligand binding. It is evident from the high negative values that ΔG_{vdW} is the driving force for the binding of compounds **5-9** within the catalytic pocket. This is in agreement with the docking result, where ΔG_{vdW} energy terms (-25.07 to -29.35 kcal mol^{-1}) also strongly favors the ligands binding. Further, the high negative values of ΔG_{VdW} and ΔG_{Lipo} shows massive hydrophobic interaction between 4A3Q and ligands **5-9**.

Table 3. The extra precision docking score and contribution to the binding free energy (MM-GBSA) (kcal mol^{-1}) between compounds 5-9 and *S.aureus* AlaR (PDB-ID: 4A3Q).

Comp	Extra-precision docking score				Contribution to the binding free energy						
	[a]gscore	[b]gemodel	[c]gecou	[d]gevdW	[e]ΔG_{Bind}	[f]ΔG_{Coul}	[g]ΔG_{Cov}	[h]ΔG_{HB}	[i]ΔG_{Lipo}	[j]ΔG_{Solv}	[k]ΔG_{vdW}
5	-5.79	-34.95	-8.53	-26.42	-36.78	-6.48	9.93	-2.41	-28.59	26.68	-39.19
6	-4.19	-34.54	-34.54	-28.74	-21.59	4.85	15.17	1.83	-21.66	8.70	-33.56
7	-3.93	-34.63	-9.55	-25.07	-59.86	-29.53	18.84	-2.05	-23.70	22.36	-42.18
8	-4.22	-35284	-5.93	-29.35	-59.07	17.33	11.42	-2.53	-41.36	6.85	-47.22
9	-4.16	-35.60	-6.81	-28.79	-80.85	-18.20	35.17	-5.68	-45.17	11.29	-57.43

Notes: [a]glide score; [b]glide model energy; [c]glide Coulomb energy; [d]glide van der Waals energy; [e]free energy of binding; [f]Coulomb energy; [g]covalent energy (internal energy); [h]hydrogen bonding energy; [i]hydrophobic energy (non-polar contribution estimated by solvent accessible surface area); [j]electrostatic solvation energy; [k]van der Waals energy.

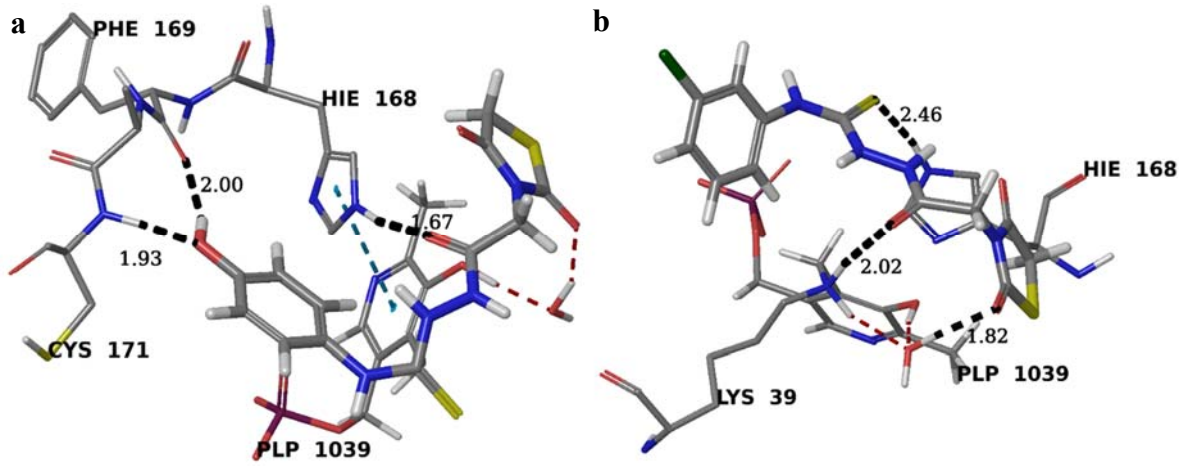

Figure 4. The extra-precision docked pose of, a) compound 7, and b) 8, within the catalytic pocket of AlaR (PDB-ID: 4A3Q).

Induced fit docking (IFD)

To further quantify the binding affinity of the active molecule **8** at the catalytic pocket of AlaR *S. aureus*, induced fit docking study was performed. In the induced fit docking (IFD), the molecule **8** had an IFD docking score of -5.286 kcal mol^{-1}. Among the sixty nine generated docked poses, the pose with highest IFD score (-21771 kcal mol^{-1}) was selected for MD simulation study. It is evident from Figure 5a that binding pose observed in the induced fit docking is relatively different from the extra-precision docking pose. The molecule **8** showed one hydrogen bonding interaction between the position four keto group of 2,4-thiazolidinedione and thiol group of Cys171 (>C=O···SH, 2.39 Å) while the phenyl ring established a π-cationic interaction with the protonated -NH_2 of Lys39. The phenyl ring of compound **8** also showed a π-π stacking interaction with the phenyl ring of Tyr43 residue. These hydrophobic interactions are attractive and are responsible for further stabilization of compound within the catalytic pocket.

Molecular dynamics simulation

In order to get an insight about the binding mode and stability, molecular dynamics (MD) simulation was performed for the induced fit docked complex **8**/4A3Q. The root mean square deviations (RMSDs) of protein backbone, C-*α* and heavy atoms of the MD trajectory were calculated (Supplementary Figure S4). During last 10 ns of simulation, the RMSD values observed for the complex backbone, C-α and heavy atom became stable in the range 1.50-2.02, 1.52-2.02 and 1.8-2.42 Å, respectively. The major fluctuations were observed in the region Ala172-Pro175 present on loop (Thr167-Asp177) connecting *β*-sheet (Leu160-Phe166) and *α*-helix (Met178-Asn191); Gln258-Thr272 present on loop (Leu257-Thr275) connecting *β*-sheet (Gln253-Thr256) and other *β*-sheet (Thr276-Leu280). The radius of gyration (rGyr) for all the backbone (blue circle) and C-*α* (red triangle) atoms as functions of the MD simulation time is represented in Supplementary Figure S5. The rGyr of both backbone and C-*α* atoms of **8**/4A3Q complex were in the range 23.78-24.21 and 23.55-24.10 Å, respectively indicating that whole system is in rexaled conformation. During MD simulation hydrogen bonding, *π*-cation interaction and *π*-*π* stacking were observed within the region Lys39-Tyr43, Met136-Asp173 and Ser204-Pro229, whereas no interactions were observed in the flexible region Gly44-Thr134 and Glu231-Asn353. Protein backbone and C-*α* atoms of catalytic domain residues which are binding to the ligand showed RMSF values in the range 0.38-1.51 and 0.37-1.61 Å, respectively (Supplementary Figure S6), indicating low fluctuations of these residues and this is in correlation with the B-factor (8.48-42.82 Å^2) of these residues. Compared to the protein crystal structure average B-factor (21.0 Å^2), a little higher average B-factor of 30.83 Å^2 was observed for the catalytic pocket residues during MD simulation. Analysis of simulation trajectory of **8**/4A3Q complex showed five residues Lys39, Arg138, His168, Cys171 and Tyr354 anchoring into the binding pocket of AlaR (Figure 5b also Supplementary Figure S7 and S8). A strong π-π stacking (60% of MD simulation) was observed between *p*-chlorophenyl ring and Tyr354 residue. A moderate frequency salt bridge interaction (27% of MD simulation) was also observed between *p*-chlorophenyl ring and Lys39 residue. These interactions are in correlation with our induced fit docking result (Figure 5a). Further, carbonyl oxygen of thiazolidine-2,4-dione ring accepted a weak hydrogen bond from Arg138 (17% of MD simulation). Low frequency (5-10% of MD simulation) water bridged interactions were also observed between ligand **8** and the residues His168, Cys171 and Tyr354. It is evident from above result that π-π stacking with Tyr354 and salt bridge interaction with Lys39 play a crucial role for the stabilization of ligand within the catalytic pocket and its inhibitory activity against AlaR enzyme. Throughout the MD simulation ligand showed RMSD and radius of gyration (rGyr) in the range 0.8 to 2.4 Å and 3.4 to 4.5 Å (Supplementary Figure S9), respectively indicating low conformational changes and high extendness of the ligand within the catalytic pocket. Between 5 to 15 ns, the solvent accessible surface area (SASA) and polar surface area (PSA) in the ranges 140-212 Å^2 and 128-150 Å^2, respectively indicated the complete burial of ligand within the catalytic pocket.

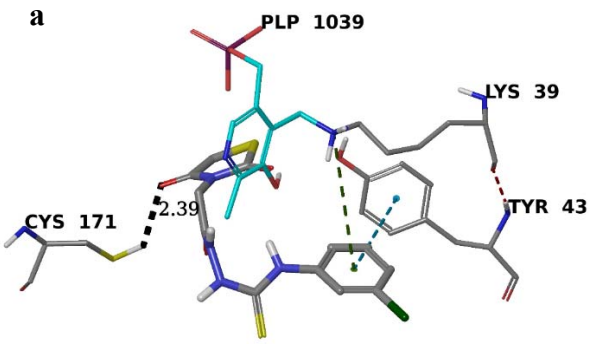

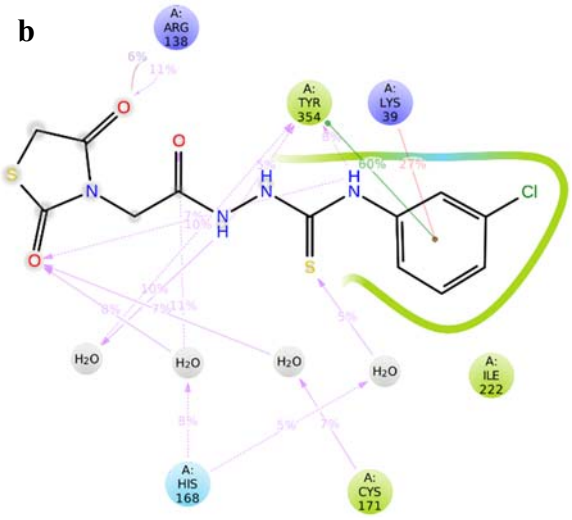

Figure 5. a) The IFD binding pose of the compound 8 within the catalytic pocket of AlaR *S. aureus* (PDB-ID: 4A3Q), b) The ligand-protein interactions during MD simulation of 8/4A3Q complex.

Experimental

General

All chemicals and solvents were of reagent grade and were purified when necessary. Melting points (mp) were determined in open glass capillaries and were uncorrected. The reaction progress was routinely monitored by thin layer chromatography (TLC) on silica gel G plates (Merck 60 F_{254}, Germany). The IR spectra were recorded on KBr disks with Schimadzu FT-IR 8400S spectrophotometer and band positions are given in cm^{-1}. The ^{1}H and ^{13}C NMR spectra were recorded using Bruker Avance-II 400 NMR spectrometer with DMSO-d_6 as solvent. Chemical shifts are reported in ppm using solvent as an internal standard. The EI-GC/MS were obtained on Thermo Scientific TSQ 8000 gas chromatograph-mass spectrometer. The elemental analyses were performed by Euro Vector CHNS Analyzer, model no: EA 3000. Arylisothiocyanates (**D_1-D_5**), were purchased from Sigma-Aldrich India, Private limited. The physicochemical properties of the synthesized compounds **5-9** are shown in Table 1. All media used in this study were purchased from Himedia, India. Methicillin, amoxicillin, *O*-acetyl-L-serine, D-alanine, *β*-nicotinamide adenine dinucleotide sodium salt, tricine were purchased from Sigma-Aldrich, India. D-cycloserine and tris base were purchased from Himedia, India. The enzyme native *G. stearothermophilus* alanine racemase was procured from Creative enzymes, USA. The enzyme L-alanine dehydrogenase was procured from Sigma-Aldrich, India.

The intermediates, 1,3-thiazolidine-2,4-dione (**1**),[35] potassium salt of 1,3-thiazolidine-2,4-dione (**2**)[35] and ethyl (2,4-dioxo-1,3-thiazolidin-3-yl)acetate (**3**)[36] were synthesized according to the reported procedure. The intermediate **3** was refluxed with hydrazine hydrate (99% w/w) in absolute ethanol and this resulted in the formation of the compound 2-(2,4-dioxo-1,3-thiazolidin-3-yl)acetohydrazide (**4**). Reaction of *p*-chlorophenyl isothiocyanate (**D_1**) with 2-(2,4-dioxo-1,3-thiazolidin-3-yl)acetohydrazide (**4**) under reflux in absolute ethanol gave compound **5**. Similarly, the compound **6** was synthesized by refluxing phenyl isothiocyanate (**D_2**) with the intermediate compound **4** in absolute ethanol. The *p*-hydroxyphenyl isothiocyanate (**D_3**) was further refluxed with 2-(2,4-dioxo-1,3-thiazolidin-3-yl)acetohydrazide (**4**) in absolute ethanol to yield compound **7** in good yield. In a similar manner, the title compounds **8** and **9** were synthesized from 3-chlorophenyl isothiocyanate (**D_4**) and *p*-tolyl isothiocyanate (**D_5**), respectively.

Synthesis of 1,3-thiazolidine-2,4-dione (1)[35]

A solution containing 56.70 g (0.6 mol) of chloroacetic acid in 60 ml of distilled water was mixed with 45.67 g (0.6 mol) of thiourea dissolved in 60 ml of distilled water and the resultant mixture was stirred (400 rpm) for 15 min. A white precipitate appeared on cooling in an ice bath. To this 60 ml of concentrated hydrochloric acid was added slowly and the resulting mixture was then refluxed with stirring (400 rpm) for 10 h. The progress of reaction was monitored by TLC. After completion of reaction the content of flask was cooled and the solid obtained was filtered, washed thoroughly with distilled water, dried and recrystallized from ethanol.

Synthesis of potassium salt of 1,3-thiazolidine-2,4-dione (2)[36]

To a solution of 1,3-thiazolidine-2,4-dione (**1**) (18.39 g, 0.157 mol) in ethanol (30 ml), a solution of potassium hydroxide (9.71 g, 0.173 mol) in ethanol (23 ml) was added. The mixture was stirred (300 rpm) for 2 h and then cooled in an ice-bath. The separated crystalline solid was filtered, washed with ethanol, dried and recrystallized from ethanol.

Synthesis of ethyl (2,4-dioxo-1,3-thiazolidin-3-yl)acetate (3) [36]

To a suspension of potassium salt of 1,3-thiazolidine-2,4-dione (**2**) (10.24 g, 0.066 mol) in dimethylformamide (35 ml), 7.06 ml of ethyl chloroacetate (0.066 mol) was added slowly. The resulting mixture was then refluxed with stirring (400 rpm) for 10 h. After completion of reaction, the reaction mixture was poured into ice cold water (200 ml). The product separated as reddish orange liquid. The oil was taken up in chloroform (20 ml), washed three times with distilled water, and dried over anhydrous sodium sulphate. Solvent was removed under reduced pressure and the residual oil was distilled out.

Synthesis of 2-(2,4-dioxo-1,3-thiazolidin-3-yl) acetohydrazide (4)

To a solution of ethyl (2,4-dioxo-1,3-thiazolidin-3-yl)acetate (**3**) (16.66 g, 0.082 mol) in absolute ethanol (10 ml) was added 4 ml hydrazine hydrate (0.082 mol, 99% w/w). The resultant mixture was heated under reflux for 6 h and then allowed to cool at room temperature. The precipitate thus obtained was filtered, dried and recrystallized from ethanol.

General procedure for the synthesis of 2-[(2,4-dioxo-1,3-thiazolidin-3-yl)acetyl]-*N*-arylhydrazinecarbothioamides (5-9)

A mixture of 2-(2,4-dioxo-1,3-thiazolidin-3-yl)acetohydrazide (**4**) (0.95 g, 0.005 mol) and the corresponding phenyl isothiocyanates (**D_1-D_5**) (0.005 mol) in ethanol (20 ml) was heated under reflux for 10-13 h. The progress of reaction was monitored by TLC. After completion of reaction, mixture was cooled to the room temperature and the precipitated solid was filtered, washed thoroughly with cold ethanol, dried and recrystallized from appropriate solvent to yield compounds **5-9**.

Determination of minimum inhibitory concentration (MIC)

To characterize the antibacterial activity of test compounds, we used Gram-positive bacteria *S. aureus* (ATCC 6538P, ATCC 25923 and ATCC 29213) and *B. subtilis* (NCIB 8054) and Gram-negative bacteria *P. aeruginosa* (ATCC 19429), *E. coli* (ATCC 8739) procured from the National Chemical Laboratory, Pune, India. The cultures were started from the transference of stock cultures for Mueller-Hinton broth at 37 °C for a period of 24 h. The viability of bacteria was estimated through the pour-plate technique utilizing the agar medium with populations in concentrations higher than 10^7 CFU/mL. Eight dilutions (0.78, 1.5625, 3.125, 6.25, 12.5, 25, 50, and 100 µg/ml) of test compounds and standard drugs methicillin and amoxycillin were prepared in sterile millipore double distilled water. The MIC values were determined by broth dilution method in culture tubes as per the guidelines of Clinical and Laboratory Standards Institute with some modifications.[37] A positive control test was performed using the inoculated broth supplemented with the same volume of DMSO as used for the test and standard compounds. Testing was carried out in Mueller-Hinton broth at pH 7.4 using two fold serial dilution technique. Tube containing only Mueller-Hinton broth was used as negative control. After incubation for 24 h at 37 °C, the tubes with no visible growth of microorganism were recorded to represent the MIC and expressed in µg/ml. Every experiment was replicated thrice (Table 2).

AlaR enzyme inhibitory assay

The *G. stearothermophilus* AlaR inhibitory assay performed was based on the conversion of D-Ala to L-Ala by the AlaR enzyme followed by deamination of L-Ala to

pyruvate by NAD-dependent-L-Ala dehydrogenase.[52] The NADH formation in the reaction was estimated fluorimetrically by excitation and emission wavelength at 340 nm and 460 nm respectively. The synthesized compounds and the standards were screened at ten different concentrations ranging from 0.19 µg/ml to 100 µg/ml. The stock solutions were prepared in dimethyl sulphoxide. As per the protocol, the stock solution of AlaR enzyme (1 mg/ml) was diluted to 1:100 in 50 mM tris pH 7.5 on ice. The 20 µl of diluted *G. stearothermophilus* AlaR enzyme and 5 µl of compound was then added into a well of 384-well black plate. The plate was then incubated for 60 min. The reaction cocktail containing 20 mM tricine pH 8.5, 20 mM *β*-nicotinamide adenine dinucleotide, 0.15 U/ml L-alanine dehydrogenase and 0.1 mM D-Ala, was dispensed (25 µl) into each well. The plates were again incubated for 15 min. The fluorescence intensity was measured at 340 nm/460 nm excitation/emission. Percent inhibition at each inhibitor concentration was calculated with respect to a positive control with no inhibitor. The results were fitted onto a sigmoidal dose-response curve to calculate the IC_{50} (compound concentration that causes 50% inhibition)[38] using Prism™ 5 software (GraphPad). Results are expressed in mean ±SD (n = 3).

Compound cytoxicity studies by sulforhodamine B assay

The well-known sulforhodamine B assay for determining cell viability was used to characterize the cytotoxic effect of different concentration of compounds on mouse fibroblast cell line L929. Sulforhodamine B is an anionic dye that binds to protein electrostatically. The fixed dye was measured photometrically at 540 nm after solubilization which correlates with the total protein synthesis and thus cell proliferation. Normal mouse fibroblast cell line L929 was obtained from National Centre for Cell Science, (NCCS) Pune, India. The mouse fibroblast cell line was maintained in Dulbecco's modified Eagle's medium (DMEM) and supplemented with 10% foetal bovine serum, sodium bicarbonate and antibiotic solution (100 units of penicillin, 100 µg of streptomycin, and 0.25 µg of amphotericin B per ml). Cells were maintained in 25 cm^2 tissue culture flasks at 37 °C in a humidified atmosphere of 5% CO_2 and 95% air. Stock solutions of the different compounds were prepared in 100% DMSO and the final concentration of DMSO was maintained at 0.1% in all the cell culture experiments. The percentage of viable cells was determined by the standard sulforhodamine B (SRB) assay. Briefly, 0.5 x 10^5 cells/mL were seeded in 96 well cell culture plate and incubated for 24 h. After 24 h of incubation, the old media was discarded and replaced with fresh media containing either vehicle (0.1% DMSO) or different concentration of drug (50, 100 and 150 µM) and incubated for additional 24 h. After 24 h of compound exposure, cells were fixed in ice cold 10% trichloroacetic acid and stained with anionic SRB dye.[39]

Molecular docking and binding free energy calculation using Prime/MM-GBSA approach

The 3-Dimensional structure of ligands were sketched in the buider panel of Maestro v11.7 (Schrödinger suite 2017-3, LLC, New York, NY) and prepared by Ligprep module with optimized potential for liquid simulations (OPLS3) force field.[40] The low energy conformation of each ligand was used for the docking study. The 3D crystal structure of the mutant *S. aureus* AlaR enzyme (PDB-ID: 4A3Q, resolution: 2.15 Å) was retrieved from the protein data bank and prepared by the Protein Preparation Wizard tool.[41] The protein structure was pre-processed to assign the bond orders and zero order bonds to metals. The missing side chains were added and breaks in protein structure was repaired with prime (v4.9).[42] Energy minimization was performed with OPLS3 force field[40] and crystallographic water molecules with less than three hydrogen bonds were deleted. H-bonds were assigned keeping the crystal symmetry and minimization of hydrogens of altered species was kept as default. Finally, the restrained minimization was performed until the convergence of heavy atoms reached to 0.30 Å RMSD. The active site was defined with a 10 Å

radius around the Lys39 residue and a grid box was generated. In Ramachandran plot (Supplementary Figure S1) all residues were observed to be in the allowed region except glycine. Low energy conformations of all ligands were docked into the catalytic pocket of the prepared protein using grid based ligand docking with energetics (Glide v7.6)[43] (Table 3). Glide docking was performed in XP mode without applying any constraints. Local optimization feature in Prime (v4.9)[42] was used to minimize the docked poses and binding free energies of docked complexes were computed using the MM-GBSA continuum solvent model which incorporates the OPLS3 force field,[40] VSGB 2.0 implicit solvent model[44] and rotamer search algorithms (Table 3).

Induced fit docking

The preparted protein structure of 4A3Q was used for IFD studies incorporated in the Schrödinger software suite. 10 Å 3D grid box was generated with the centre defined by the Lys39 residue. The prepared ligand was docked into the study model using the Schrödinger IFD protocol with extended sampling. It uses Glide module to account for the ligand flexibility and the refinement module in Prime to account for the receptor flexibility. The scaling factor was set to 0.5 to soften the potentials of the receptor and ligand and a maximum of 20 poses was saved. The IFD scores, that accounts for both the protein-ligand interaction energy and the total energy of the system was calculated. IFD pose showing highest score (-21771 kcal mol^{-1}) was further used for the MD simulation.

Molecular dynamics simulation

The molecular dynamics[45] studies for AlaR-inhibitor complex (**8**/4A3Q) was performed in an explicit solvent milieu using the TIP4P water model[46] with OPLS3 force field[40] using Desmond software (v5.1). The ligand bound receptor complexes were solvated with water molecules in an orthorhombic box (volume 4A3Q = 514517 $Å^3$) allowing for a 10 Å buffer region between protein atoms and box sides. Overlapping water molecules were deleted and the systems were neutralized by the addition of counter ions (Na^+). The total numbers of atoms in solvated protein structure for the MD simulations were 49509 for 4A3Q (including 14460 water molecules). The total number of atoms of 4A3Q with the substrate was approximately 6018. Each system was placed at a distance of 10 Å from the edge of the box and LBFGS minimization was performed with 3 vectors and with minimum 10 steepest descent steps until a gradient threshold of 25 kcal mol^{-1} $Å^{-1}$ was reached. The maximum iterations during minimization were 2000 and convergence threshold was kept at 1.0 kcal mol^{-1} $Å^{-1}$. For long range electrostatic interactions, smooth particle mesh Ewald[47] method was used at a tolerance of 1e-09 and a cut-off radius of 9 Å was selected for short range electrostatic interactions. Before equilibration and MD simulations, systems were minimized and pre-equilibrated using the default relaxation routine implemented in Desmond. Each system was gradually heated in the NPT ensemble to 300 K with a time step of 2 fs. For MD, a multiple timestep RESPA integration algorithm was used throughout the simulation with time steps of 2, 2 and 6 fs for bonded, 'near' non-bonded, and 'far' non-bonded interactions respectively. A 15 ns MD simulation in the NPT ensemble (T = 300 K, thermostat relaxation time = 100 ps; P = 1 atm; barostat relaxation time = 100 ps) was performed using a Nose-Hoover thermostat[48] and Martyna-Tobias-Klein barostat.[49] Data were collected every 100 ps during MD run. 3D structures and trajectories were visually inspected using the Maestro graphical interface.

Conclusion

Some novel 2-[(2,4-dioxo-1,3-thiazolidin-3-yl)acetyl]-*N*-arylhydrazinecarbothioamides (**5-9**) were synthesized and characterized by spectral data like FT-IR, ^{1}H NMR, ^{13}C NMR, mass spectra and elemental analysis. The results of *in vitro* antibacterial studies suggested that the synthesized molecules have significant antibacterial activity against the selected strains. The MIC studies of compound **8** showed

promising activity towards the selected strain of *B. subtilis* and moderate inhibitory activity towards the selected strains of *S. aureus*, *P. aeruginosa* and *E. coli*. The AlaR enzyme inhibitory assay of tested compounds **7** and **8** showed promising inhibitory activity (IC_{50} = 0.5 and 1.8 μM respectively) when compared to the standard D-cycloserine (IC_{50} = 0.93 μM) and *O*-acetyl-L-serine (IC_{50} = 4.2 μM). The compounds cytotoxic effect on mouse fibroblast cell line L929 was studied by sulforhodamine B assay and the test compounds showed no significant effect on the cell viability and had minimal cytotoxic effect even at a higher concentration (150 μM). For compounds **5-9** extra-precision molecular docking was performed and binding free energy were calculated by MM-GBSA approach. It is evident from result that ΔG_{vdW} is the driving force for the binding of compounds **5-9** within the catalytic pocket of *S. aureus* AlaR enzyme. Further, induced fit docking was carried out for compound **8** and a 15 ns molecular dynamics simulation was performed using the induced fit docked complex **8**/4A3Q to get further insight into the binding mode of **8** with *S. aureus* AlaR enzyme. It was evident from the molecular docking and molecular dynamics results that hydrophobic interactions play crucial role for the stabilization of inhibitor within the catalytic pocket of *S. aureus* AlaR enzyme. The synthesized compound **8** can be considered as a promising antibacterial agent and may also serve as potent lead molecule for further antibacterial drug discovery and development.

Acknowledgments

Authors would like to thank the University Grants Commission (UGC), Government of India, for the financial support (No. F1-17.1/2014-15/RGNF-2014-15-SC-KER-61880).

Supplementary material

Synthesis, biological evaluation and molecular modeling studies of some novel 2-[(2,4-dioxo-1,3-thiazolidin-3-yl)acetyl]-*N*-arylhydrazinecarbothioamides as antibacterial agents targeting alanine racemase enzyme

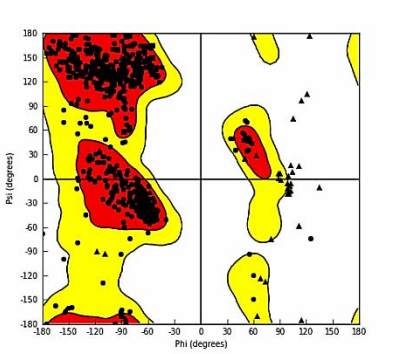

Figure S1. The Ramachandran plot of *S. aureus* AlaR (PDB-ID: 4A3Q).

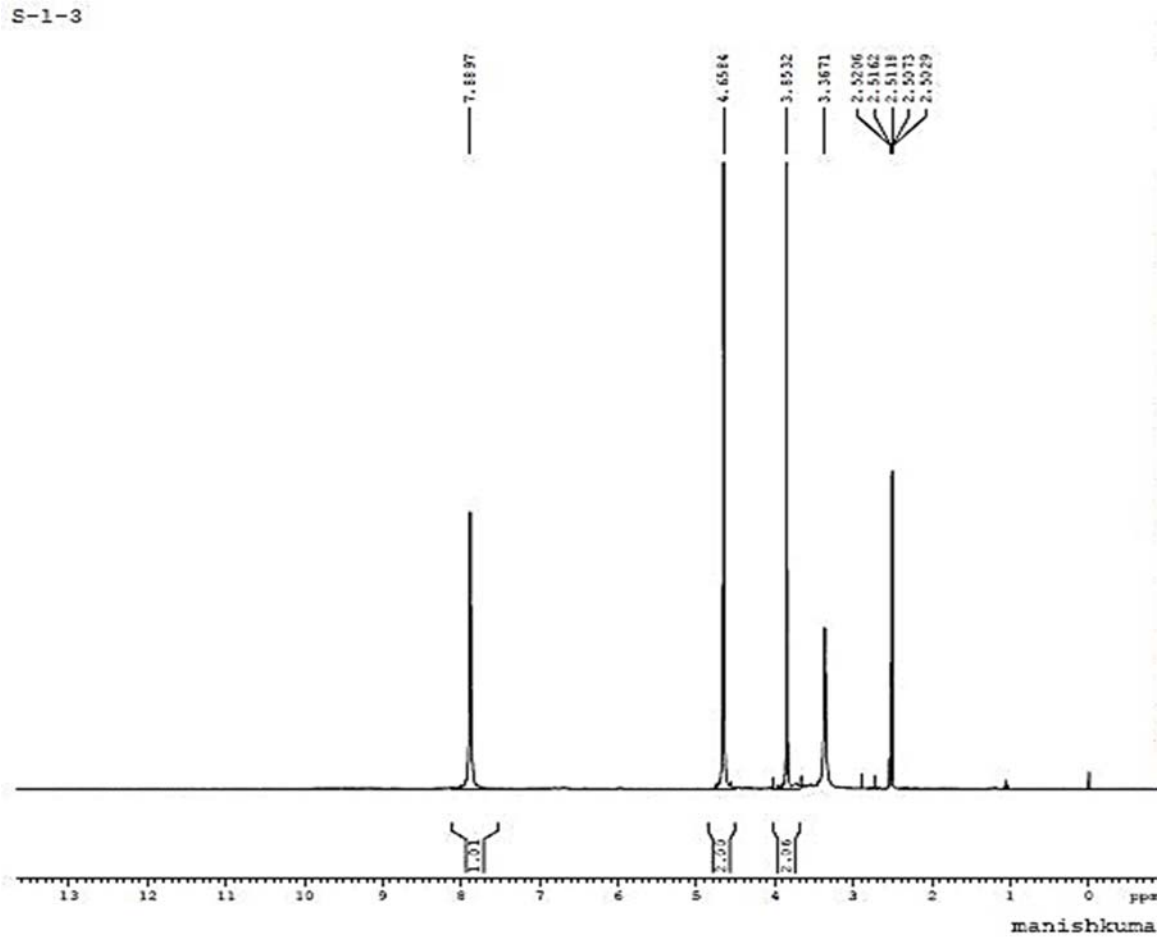

Figure S2.[1]H NMR spectrum of 2-(2,4-dioxo-1,3-thiazolidin-3-yl)acetohydrazide (4).

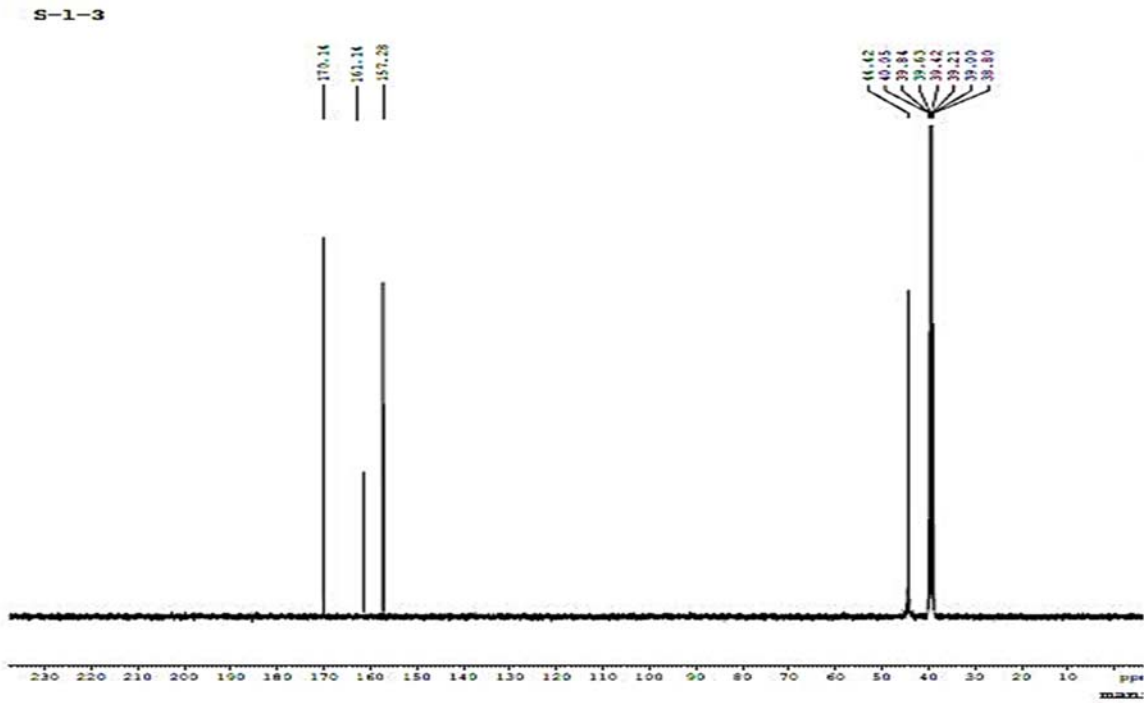

Figure S3.^{13}C NMR spectrum of 2-(2,4-dioxo-1,3-thiazolidin-3-yl)acetohydrazide (4).

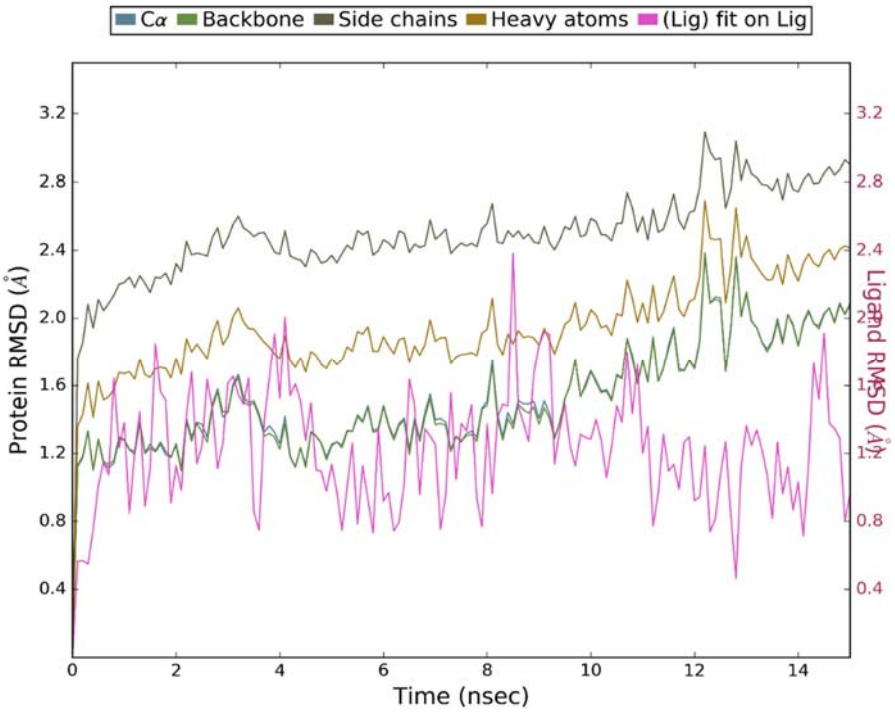

Figure S4. The Root mean square deviation (RMSD) for 8/4A3Q complex during MD simulation.

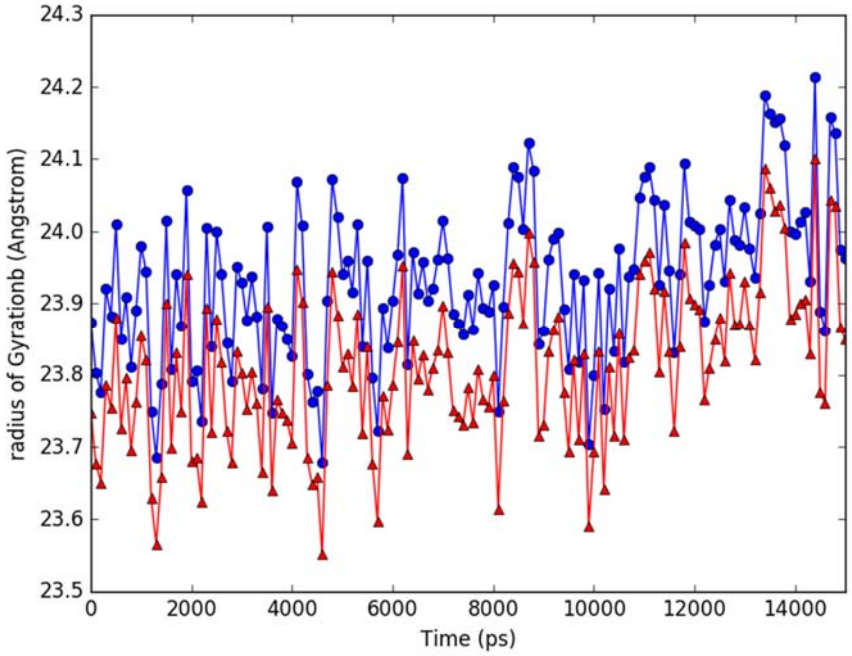

Figure S5. Represent radius of gyration for all the backbone (blue circle) and C-α (red triangle) atoms as functions of the MD simulation of 8/4A3Q complex.

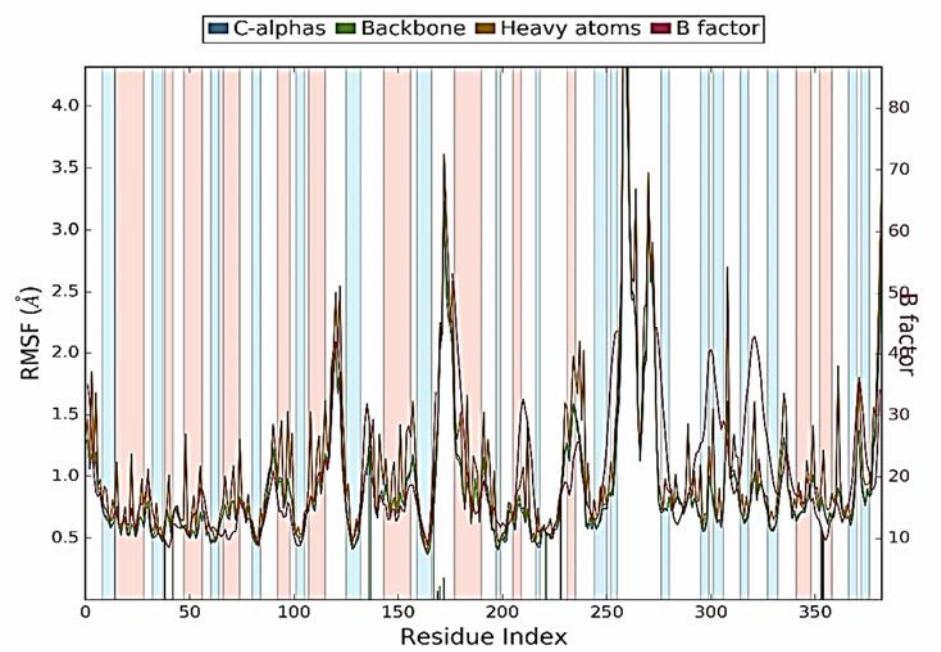

Figure S6. The Root mean square fluctuation (RMSF) for 8/4A3Q complex during MD simulation.

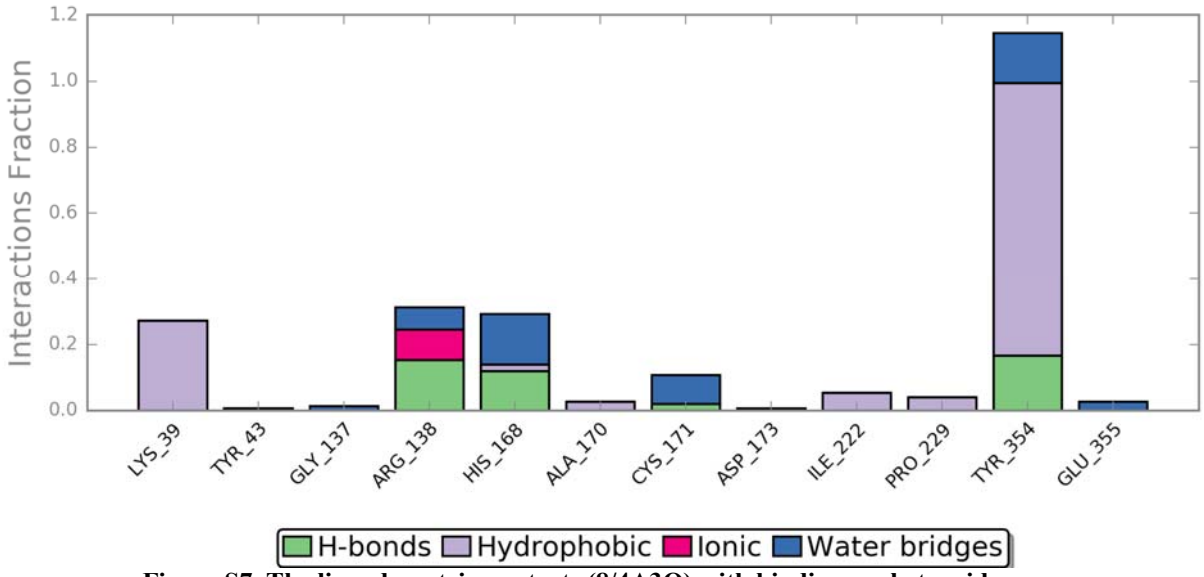

Figure S7. The ligand-protein contacts (8/4A3Q) with binding pocket residues.

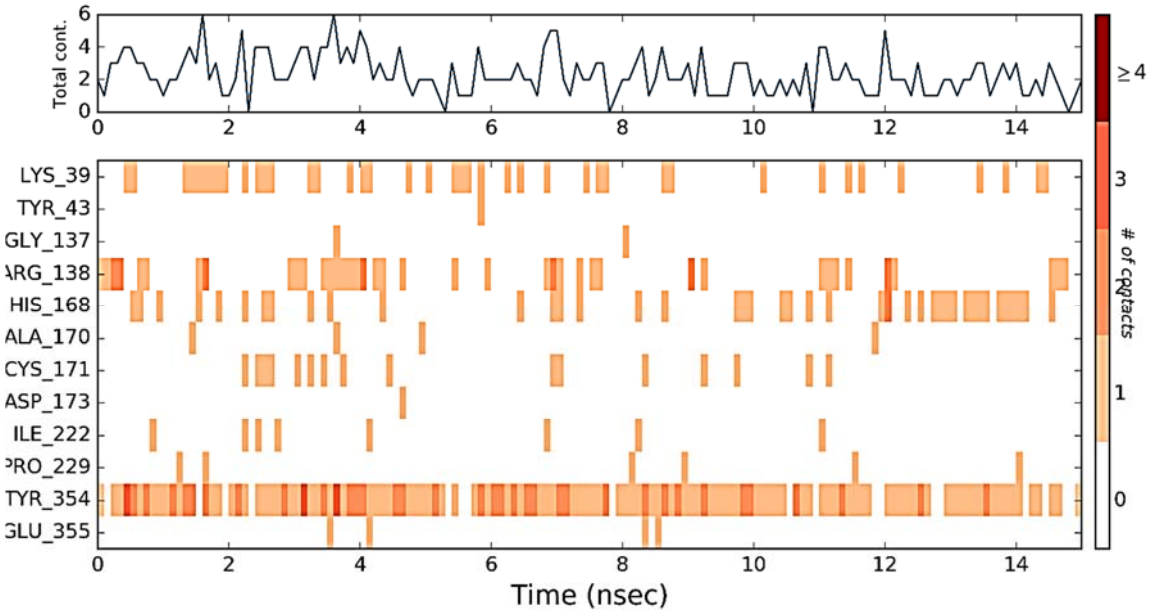

Figure S8. The ligand-protein contacts (8/4A3Q) with binding pocket residues during 15 ns MD simulation.

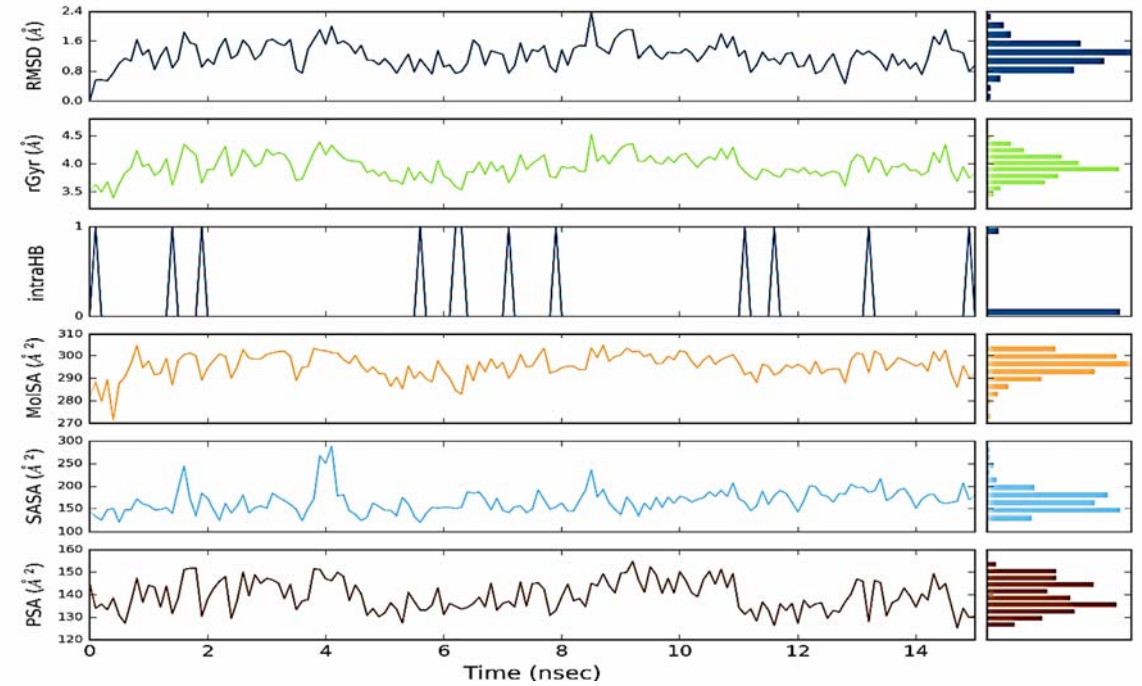

Figure S9. The Ligand interaction properties. RMSD: Root mean square deviation of a ligand with respect to the reference conformation; rGyr: Radius of gyration which measures the 'extendedness' of a ligand; intraHB: Intramolecular hydrogen bonds; MolSA: Molecular surface area; SASA: Solvent accessible surface area; PSA: Polar surface area.

REFERENCES

(1) Hanaki H., Labischinski H., Sasaki K., Kuwahara-Arai K., Inaba Y. and Hiramatsu K. Mechanism of vancomycin resistance in MRSA strain Mu50 Jpn. J. Antibiot. 1998; 51: 237-247.

(2) Lin Y. H., Wu V. C., Tsai I. J., Ho Y. L., Hwang J. J., Tsau Y. K., Wu C. Y., Wu, K. D. and Hsueh PR. High frequency of linezolid-associated thrombocytopenia among patients with renal insufficiency. Int. J. Antimicrob. Agents. 2006; 28:345-351.

(3) Echevarria K., Datta P., Cadena J. and Lewis J. S. Severe myopathy and possible hepatotoxicity related to daptomycin. J. Antimicrob. Chemother. 2005; 55:599-600.

(4) Skiest D. J. Treatment failure resulting from resistance of Staphylococcus aureus to daptomycin. J Clin. Microbiol. 2006; 44:655-656.

(5) Wilson P., Andrews J. A., Charlesworth R., Walesby R., Singer M., Farrell D. J. and Robbins M. Linezolid resistance in clinical isolates of Staphylococcus aureus. J. Antimicrob. Chemother. 2003; 51:186-188.

(6) Walsh C. T. Enzymes in the D-alanine branch of bacterial cell wall peptidoglycan assembly. J. Biol. Chem. 1989; 264:2393-2396.

(7) Saito M., Nishimura K., Hasegawa Y., Shinohara T., Wakabayashi S., Kurihara T., Ishizuka M. and Nagata Y. Alanine racemase from Helicobacter pylori NCTC 11637: purification, characterization and gene cloning. Life Sci. 2007; 80:788-794.

(8) Strych U., Huang H. C., Krause K. L. and Benedik M. J. Characterization of the Alanine Racemases from Pseudomonas aeruginosa PAO1. Curr. Microbiol. 2000; 41:290-294.

(9) Thompson R. J., Bouwer H. G., Portnoy D. A. and Frankel, F. R. Pathogenicity and Immunogenicity of a Listeria monocytogenes Strain That Requires D-Alanine for Growth Infect. Immun. 1998; 66:3552-3561.

(10) Watanabe A., Yoshimura T., Mikami B., Hayashi H., Kagamiyama H. and Esaki N. Reaction Mechanism of Alanine Racemase from Bacillus stearothermophilus. J. Biol. Chem. 2002; 277:19166-19172.

(11) Scaletti E. R., Luckner S. R. and Krause K. L. Structural features and kinetic characterization of alanine racemase from Staphylococcus aureus (Mu50). Acta Crystallogr. Sect. D Biol. Crystallogr. 2012; 68:82-92.

(12) LeMagueres P., Im H., Ebalunode J., Strych U., Benedik M. J., Briggs J. M., Kohn H. and Krause K. L. The 1.9 A crystal structure of alanine racemase from Mycobacterium tuberculosis contains a conserved entryway into the active site. Biochemistry. 2005; 44:1471-1481.

(13) Fenn T. D., Holyoak T., Stamper G. F. and Ringe D. Effect of a Y265F mutant on the transamination-based cycloserine inactivation of alanine racemase. Biochemistry. 2005; 44:5317-5327.

(14) Au K., Ren J., Walter T. S., Harlos K., Nettleship J. E., Owens R. J., Stuart D. I. and Esnouf R. M. Structures of an alanine racemase from Bacillus anthracis (BA0252) in the presence and absence of (R)-1-aminoethylphosphonic acid (L-Ala-P) Acta Crystallogr. Sect. F Struct. Biol. Cryst. Commun. 2008; 64:327-333.

(15) Priyadarshi A., Lee E. H., Sung M. W., Nam K. H., Lee W. H., Kim E. E. and Hwang K. Y. Structural insights into the alanine racemase from Enterococcus faecalis. Biochim. Biophys. Acta. 2009; 1794:1030-1040.

(16) Im H., Sharpe M. L., Strych U., Davlieva M. and Krause K. L. The crystal structure of alanine racemase from Streptococcus pneumoniae, a target for structure-based drug design. BMC Microbiol. 2011; 11:116.

(17) Asojo O. A., Nelson S. K., Mootien S., Lee Y., Rezende W. C., Hyman D. A., Matsumoto M. M., Reiling S., Kelleher A., Ledizet M., Koski R. A. and Anthony K. G. Structural and biochemical analyses of alanine racemase from the multidrug-resistant Clostridium difficile strain 630. Acta Crystallogr. D Biol. Crystallogr. 2014; 70:1922-1933.

(18) Tassoni R., van der Aart L. T., Ubbink M., van Wezel G. P. and Pannu N. S. Structural and functional characterization of the alanine racemase from Streptomyces coelicolor A3(2). Biochem. Biophys. Res. Commun. 2017; 483:122-128.

(19) Copie V., Faraci W. S., Walsh C. T. and Griffin R. G. Inhibition of alanine racemase by alanine phosphonate: detection of an imine linkage to pyridoxal 5'-phosphate in the enzyme-inhibitor complex by solid-state nitrogen-15 nuclear magnetic resonance Biochemistry. 1988; 27:4966-4970.

(20) Yew W. W., Wong C. F., Wong P. C., Lee J. and Chau C. H. Adverse neurological reactions in patients with multidrug-resistant pulmonary tuberculosis after coadministration of cycloserine and ofloxacin. Clin. Infect. Dis. 1993; 17:288-289.

(21) Neuhaus F. C. Selective inhibition of enzymes utilizing alanine in the biosynthesis of peptidoglycan. Antimicrob. Agents Chemother. 1967; 7:304-313.

(22) Wang E. and Walsh C. Suicide substrates for the alanine racemase of Escherichia coli B. Biochemistry. 1978; 17:1313-1321.

(23) Faraci W. S. and Walsh C. T. Mechanism of inactivation of alanine racemase by β-β-β-trifluoroalanine. Biochemistry.1989; 28:431-437.

(24) Chen J., Zhang S., Cui P., Shi W., Zhang W. and Zhang Y. Identification of novel mutations associated with cycloserine resistance in Mycobacterium tuberculosis. J Antimicrob. Chemother. 2017; 72:3272-3276.

(25) Stamper G. F., Morollo A. A. and Ringe D. Reaction of alanine racemase with 1-aminoethylphosphonic acid forms a stable external aldimine. Biochemistry. 1998; 37:10438-10445.

(26) Azam M. A., Jayaram U. Inhibitors of alanine racemase enzyme: a review. J. Enzyme Inhib. Med. Chem. 2016; 31: 517-526.

(27) Tuncbilek M. and Altanlar N. Synthesis of New 3□(Substituted Phenacyl)□5□[3′□(4H□4□oxo□1□benzopyran□2□yl)□benzylidene]□2,4□thiazolidinediones and their Antimicrobial Activity. Arch. Pharm. 2006; 339:213-216.

(28) Bahare R. S., Ganguly S., Choowongkomon K. and Seetaha S. Synthesis, HIV-1 RT inhibitory, antibacterial, antifungal and binding mode studies of some novel N-substituted 5-benzylidine-2,4-thiazolidinediones. Daru. 2015; 23:6.

(29) Moorthy P., Ekambaram S. P. and Perumal S. S. Synthesis, characterization and antimicrobial evaluation of imidazolyl thiazolidinedione derivatives. Arab J. Chem. 2014; 8:10.

(30) Parekh N. M., Juddhawala K. V. and Rawal B. M. Antimicrobial activity of thiazolyl benzenesulfonamide-condensed 2,4-thiazolidinediones derivatives. Med. Chem. Res. 2013; 22:2737-2745.

(31) Liu X. F., Zheng C. J., Sun L. P., Liu X. K. and Piao H. R. Synthesis of new chalcone derivatives bearing 2,4-thiazolidinedione and benzoic acid moieties as potential anti-bacterial agents. Eur. J. Med. Chem. 2011; 46:3469-3473.

(32) Dundar O. B., Ozgen O., Mentes A., Altanlar N., Atli O., Kendi E. and Ertan R. Synthesis and antimicrobial activity of some new thiazolyl thiazolidine-2,4-dione derivatives. Bioorg. Med. Chem. 2007; 15:6012-6017.

(33) Benmohammed A., Khoumeri O., Djafri A., Terme T. and Vanelle P. Synthesis of Novel Highly Functionalized 4-Thiazolidinone Derivatives from 4-Phenyl-3-thiosemicarbazones. Molecules. 2014; 19:3068-3083.

(34) Zhang X. M., Guo H., Li Z. S., Song F. H., Wang W. M., Dai H. Q., Zhang L. X. and Wang J. G. Synthesis and evaluation of isatin-β-thiosemicarbazones as novel agents against antibiotic-resistant Gram-positive bacterial species. Eur. J. Med. Chem. 2015; 101:419-430.

(35) Pattan S., Kedar M., Pattan J., Dengale S., Sanap M., Gharate U., Shinde P. and Kadam S. Synthesis and evaluation of some novel 2,4-thiazolidinedione derivatives for antibacterial, antitubercular and antidiabetic activities. Indian J. Chem. Sec. B. 2012; 51B9:1421-1425.

(36) Lo C. P. and Shropshire E. The alkylation of 2,4-thiazolidinedione. J. Org. Chem. 1957; 22:999-1001.

(37) Barry A. L. J. The antimicrobial susceptibility test, principle and practices; ELBS: London, United Kingdom, 1999.

(38) Ciustea M., Mootien S., Rosato A. E., Perez O., Cirillo P., Yeung K. R., Ledizet M., Cynamon M. H., Aristoff P. A., Koski, R. A., Kaplan P. A. and Anthony K. G. Thiadiazolidinones: A New Class of Alanine Racemase

Inhibitors with Antimicrobial Activity against Methicillin-Resistant S. aureus. Biochem. Pharmacol. 2012; 83:368-377.

(39) Skehan P., Storeng R., Scudiero D., Monks A., McMahon J., Vistica D., Warren J. T., Bokesch H., Kenney S. and Boyd M. R. New colorimetric cytotoxicity assay for anticancer-drug screening. J. Natl. Cancer Inst. 1990; 82:1107-1112.

(40) Harder E., Damm W., Maple J., Wu C., Reboul M., Xiang J. Y., Wang L., Lupyan D., Dahlgren M. K., Knight J. L., Kaus J. W., Cerutti D. S., Krilov G., Jorgensen W. L., Abel R., Friesner RA. OPLS3: A Force Field Providing Broad Coverage of Drug-like Small Molecules and Proteins. J. Chem. Theory Comput. 2016; 12:281-296.

(41) Sastry G. M., Adzhigirey M., Day T., Annabhimoju R. and Sherman W. Protein and ligand preparation: parameters, protocols, and influence on virtual screening enrichments. J Comput. Aided Mol. Des. 2013; 27:221-234.

(42) Jacobson M. P., Pincus D. L., Rapp C. S., Day T. J., Honig B., Shaw D. E., Friesner R. A. A hierarchical approach to all-atom protein loop prediction. Proteins. 2004; 55:351-367.

(43) Friesner R. A., Murphy R. B., Repasky M. P. Frye L. L., Greenwood J. R., Halgren T. A., Sanschagrin P. C. and Mainz D. T. Extra precision glide: docking and scoring incorporating a model of hydrophobic enclosure for protein-ligand complexes. J. Med. Chem. 2006; 49:6177-6196.

(44) Li J., Abel R., Zhu K., Cao Y., Zhao S. and Friesner R. A. The VSGB 2.0 model: a next generation energy model for high resolution protein structure modeling. Proteins. 2011; 79:2794-2812.

(45) Guo Z., Mohanty U., Noehre J., Sawyer T. K., Sherman W. and Krilov G. Probing the alpha-helical structural stability of stapled p53 peptides: molecular dynamics simulations and analysis. Chem. Biol. Drug Des. 2010; 75:348-359.

(46) Jorgensen W. L., Chandrasekhar J., Madura J. D., Impey R. W. and Klein M. L. Comparison of simple potential functions for simulating liquid water. J. Chem. Phys. 1983; 79:926-935.

(47) Essmann U., Perera L., Berkowit M. L., Darden T., Lee H. and Pedersen L. G. A smooth particle mesh Ewald method. J. Chem. Phys. 1995; 103:8577-8593.

(48) Martyna G. J., Klein M. L. and Tuckerman M. Nosé-Hoover chains: The canonical ensemble via continuous dynamicsJ. Chem. Phys. 1992; 97:2635-2643.

(49) Martyna G. J., Tobias D. J. and Klein M. L. Constant pressure molecular dynamics algorithms. J. Chem. Phys. 1994; 101:4177-4189.

(50) Wardakhan W. W., El sayed N. N. and Mohareb R. M. Synthesis and anti-tumor evaluation of novel hydrazide and hydrazide-hydrazone derivatives. Acta Pharm. 2013; 63:45-57.

(51) Sun N., Li B., Shao J., Mo W., Hu B., Shen Z. and Hu X. A general and facile one-pot process of isothiocyanates from amines under aqueous conditions. Beilstein J. Org. Chem. 2012; 8:61-70.

(52) Esaki N. and Walsh C. T. Biosynthetic alanine racemase of Salmonella typhimurium: purification and characterization of the enzyme encoded by the alr gene. Biochemistry. 1986; 25:3261-3267.

التصنيع والتقييم البيولوجي ودراسه النمذجة الجزيئيه للمركب (2،4-ديوكسو-1،3-ثيازوليدين-3-يل (اسيتايل)-ن-أريل هيدرازينكاربوثيو أميد كعامل مضاد للبكتيريا يستهدف أنزيم الالنين رسيميز.

أوني جيارام[1]،محمد عزام[1] ،أشيش وادواني[2]،سمير فيرما[2]،كريشنان راثيناسامي[3]،سوسوبهان ماهانتي[3]

[1]قسم الكيمياء الصيدلانية، JSS، الهند

[2]قسم البيوتكنولوجيا الصيدلانية،JSS،الهند

[3]كلية التكنولوجيا الحيوية،المعهد الوطني للتكنولوجيا،الهند

ملخص

المضادات الحيويه تلعب دوراً مهماً في الرعايه الصحيه الحديثه. بالرغم من ذلك، يُركز دور المضادات الحيوية على علاج العدوى الطفيفه والخطيرة، ولكننا نعيش تحت تهديد كبير نتيجه انخفاض فعاليه المضادات الحيويه. حالياً، تركيز الباحثين الرئيسي هو جعل فئه جديده هيكلياً وعملياً من المضادات الحيويه .الالنين رسيميز هو انزيم بدائي واسع الانتشار يعمل كمصدر لطبقه الببتايدوجلايكن المستخدمة في تصنيع جدار الخليه البكتيريه .تهدف هذه الدراسه لتحديد بعض المثبطات الجديده لإنزيم الالنين رسيميز والتي تعمل كعامل قوي مضاد للبكتيريا .هنا نخبركم عن خمسه مركبات جديده 2-[2،4-دايكسو-1،3-ثيازوليدين-3-يل)اسيتايل]-ن-أريل هيدر ازينكاربوثيو (9،5) التي قمنا بتجميعها ووصفها بالبيانات الطيفيه .تم فحص جميع المركبات من خلال نشاطهم المضاد للبكتيريا وعملهم كمثبط لإنزيم الالنين رسميز من بكتيريا جيوباسيلز ستيروثيرموفيلس. وُجد ان مركب رقم 8 أظهر نشاط كبيراً ضد سلاله البكتيريا المختبره عند مقارنتها بدواء الميثيسيلين المعياري. عند فحص مثبطات إنزيم الالنين رسيميز، مركب رقم 8 أظهر اعلى نشاط في التثبيط (حيث أن نصف التركيز الأقصى للمثبط(IC50 =0.5mMمقارنه بالادويه المعياري للثبيط مثل د-سايكلوسيرين (IC50=0.93mM) و0-اسيتايل -ل-سيرين . (IC50=4.2mM) أثبتت دراسه السيليكو أن استبدال الكلور في حلقه الفينايل والتفاعلات المحفزه الكارهه للماء في المركب 8 تؤثر بشده في عمل تثبيط أنزيم الالنين رسيميز . تقترح الدراسه ان تصنيع المركب 8 من الممكن ان يعتبر عامل واعد اً مضاداً للبكتيريا وأيضاً من خلال جزيئاته الرصاص القويه عاملاً لزياده اكتشافات مضادات البكتيريا وتطويرها.

الكلمات الدالة: 1،3-ثيازولدين-2،4-ديون، الالنين رسيميز، نشاط مضاد البكتيريا، النمذجة الجزيئيه، التصنيع، سميه الخلايا.

تاريخ استلام البحث 2019/3/7 وتاريخ قبوله للنشر 2020/1/11.